ARTICLES

Biasing Mixed-Valence Transition Metal Complexes in Search of Bistable Complexes for Molecular Computing

Sonja B. Braun-Sand and Olaf Wiest*

Department of Chemistry and Biochemistry, University of Notre Dame, Notre Dame, Indiana 46556-5670

Received: January 25, 2003; In Final Form: June 16, 2003

Mixed-valence ruthenium complexes as possible quantum-dot cellular automata (QCA) devices are discussed with respect to the effects of a driver, or biasing charge, on the system. The hybrid density functional method B3LYP was used with a 3-21G basis set, the only all-electron basis set available for ruthenium. Three different mixed-valence complexes have been investigated as representatives of each Robin and Day class, class I, II, and III. The input and output of a QCA device is not current, but charge polarization. The more localized classes, I and II, displayed the largest amount of polarization, while the more delocalized class III complex displayed the least polarization. This type of computational analysis can be extended to study the effects of different bridging and ancillary ligands, therefore this type of analysis is useful in the design of better molecular implementations of QCA devices.

Introduction

In a recent contribution the use of mixed-valence species for quantum-dot cellular automata (QCA) was introduced.[1,2] QCA was originally proposed as islands of metal atoms composing each corner of a square on a surface.[3] When two extra electrons are added to the square, they occupy opposite corners due to Coulombic repulsion, as is shown in Figure 1. These correspond to two energetically degenerate, but distinguishable quantum states that could serve as binary code. The electrons are then able to tunnel between the two states to perform the computation, leading to possible speed increases of 100−10,000-fold over today's processors.[4] The function of a QCA device can be easily understood when considering a molecular wire, where a line of QCA cells is positioned on a surface. As shown in Figure 2, an input, or bias, on one end of the wire causes the electrons in the first cell to switch so that it is in the lowest-energy state. This induces a switch in the neighboring cell, and the signal travels down the wire like a row of falling dominoes without actual current flow. If the input is changed, all the cells in the wire will also change so that they are again in the lowest-energy configuration; therefore, the QCA idea is reliant upon ground-state configurations.

The initial demonstration of QCA used clusters of metal atoms that were in the nanometer-size range in diameter.[3] One consequence of this large size is that the system needs to be cooled to less than 1 mK to achieve function without random switching. It has been theorized that if the squares could be made smaller, approximately 20−30 Å per side, the device could function at room temperature. This is a consequence of the particle-in-a-box problem, the smaller the box, the larger the difference in energy levels and the larger the barrier to random switching. A potential problem is making clusters of metal atoms

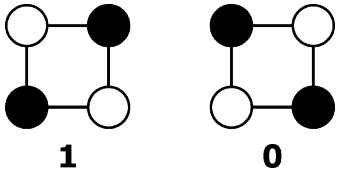

Figure 1. Bistable cell states.

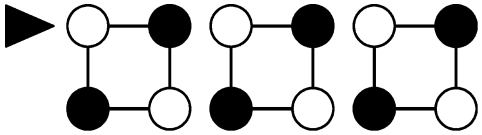

Figure 2. Input and signal down a "wire".

this small reproducibly enough to not introduce any inherent bias. However, this is a typical size of molecules, which are much easier to make reproducibly, and opens the door for possible molecular implementation of the QCA idea. A recent contribution detailed the synthesis of a "Creutz−Taube square," which could effectively replace each cluster of metal atoms with a single ruthenium atom.[5] This work examines bisruthenium analogues of the Creutz−Taube complex, which could function as QCA devices. Since the Coulombic interaction responsible for the biasing process depends only on the charges and the distance between them, we represent the four-dot cell by the conceptually identical,[1] but computationally much less time-consuming, bisruthenium complexes.

Our previous work explored the intracell communication in mixed-valence transition metal species.[6] A study of the geometric and electronic structures of three mixed-valence ruthenium dimers was done using ab initio Hartree−Fock and hybrid density functional methods at the HF/3-21G and B3LYP/3-21G levels of theory. These complexes were representatives of the Robin and Day classes I, II, and III. Predicted geometries were

* To whom correspondence should be addressed. E-mail: owiest@nd.edu.

10.1021/jp034208t CCC: $25.00
Published on Web 08/16/2003

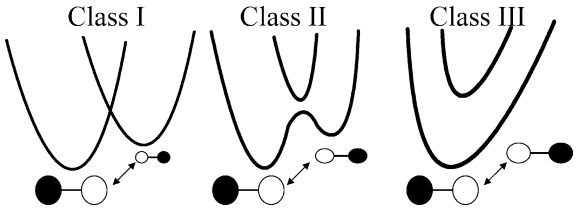

Figure 3. Schematic potential energy surfaces for electron transfer in classes I, II, and III when the system is biased.

compared to experimental data as well as previous computational studies. The B3LYP method predicted structures in better agreement with experiment than the HF method. The analysis of the orbital energies and localization provided insights into the degree of localization and the Robin−Day classification. They are therefore useful tools for the design of mixed-valence compounds for use in molecular QCA.

The present work explores the interactions of these systems with a biasing charge using electronic structure methods and is, to the best of our knowledge, the first such study. Robin and Day have divided mixed-valence compounds into three different classes, class I, class II, and class III.[7] When a bias, such as a charge, is added to these systems, it perturbs the potential energy surfaces so that one electronic configuration is lower in energy than the other (the extra electron is energetically favored to localize on one ruthenium and not the other). This biasing charge is also called a driver, because it "drives" the potential energy surface of the system so that one electronic configuration is now favored. This is shown schematically in Figure 3. This biasing in favor of one electronic structure over another is essential for the function of QCA, so that computation can be done and output can be read. Also essential for computation is the ability to switch back and forth between the two possible states many times. It is possible that either class II or III could function as QCA devices because these have a fast rate of electron transfer for fast computation, yet when biased have barriers to electron transfer high enough that unwanted switching would not occur at room temperature. Ideally, this bistability would exhibit a nonlinear response, switching sharply between the "1" and "0" state, to minimize any ambiguity in reading the output. We have calculated this response in three mixed-valence complexes in this work, representative of each Robin and Day class.

Model Systems. Two models were examined for the electron polarization. The first, which we have termed "end-on" in this work, places a lithium cation parallel to the ruthenium−ruthenium axis, as shown in Figures 4−6. This is done to mimic the polarization of a QCA cell induced by the polarization of the neighboring QCA cell, as would be the case in a QCA wire of two-dot cells, where the closest contact between two adjacent cells are the endpoints. The second model, which we have termed "side-on," also places a lithium cation parallel to the ruthenium−ruthenium axis, but it is placed below the complex, as shown in Figures 7−9. This is to mimic the polarization that would occur within a four-dot QCA cell. We chose to use this model rather than the complete square because computationally it is more efficient.

Mixed-valence ruthenium complexes were chosen to represent the three Robin−Day classes. Class III, the strongest coupled case, is represented by the well-known Creutz−Taube complex, decaammine(μ-pyrazine)diruthenium(5+), **1**.[8−10] Class III complexes have a very small barrier to electron transfer, and ultrafast rates. Class II complexes are represented by decaammine(μ-4,4′-bipyridine)diruthenium(5+), **2**.[11−15] Class II complexes are the most likely to have a barrier low enough that it can switch when induced yet be able to maintain "1" or "0" states without undesirable random electron transfer. Decaammine(μ-piperazine)diruthenium(5+), **3**, was chosen as the example for a class I compound, even though **3** has not yet been described in the literature. **3** was chosen because of its analogous structure to **1** and absence of π bonds. For class I complexes, the barrier to electron transfer is very high, such that the complex is permanently "locked" in one position. The use of transition metal complexes is attractive because the electronic properties can be tuned by varying the bridging as well as the ancillary ligands.

Computational Details

All calculations were performed using the Gaussian-98 series of programs.[16] For consistency with the previous work,[6] DFT was used. Gradient-corrected DFT has been used previously to describe the properties of mixed-valence complexes, with both localized[17] and delocalized[18] electrons. Specifically, the Creutz−Taube complex has previously been calculated using DFT.[6,19,20] However, pure DFT methods are known to be biased toward delocalized structures. This can be countered by admixture of HF exchange. The resulting hybrid DFT methods typically perform significantly better than nonlocal DFT methods, especially with respect to the counterplay of localized and delocalized structures in radical ions.[21−25] Therefore, the hybrid DFT method B3LYP was chosen. B3LYP has been shown to perform well with many difficult chemical problems, including open-shell transition metal chemistry; therefore, all structures were fully optimized and characterized at the B3LYP level of theory with a 3-21G basis set on all atoms, including ruthenium. The degeneracy problem should be less of an issue for the structures under study here, because the bias introduced by the lithium ion should cause any degeneracy to be broken. Symmetry was not imposed on any of the complexes. The 3-21G basis set was chosen as a reasonable compromise between the accuracy and size of the calculation. It is also the only all-electron basis set available for ruthenium. The polarization of the complexes was gauged using Mulliken charges. Basis-set-derived population analyses (such as Mulliken charge) are most useful for trend comparison, as used here, rather than an estimate of the actual value.[26] The geometries were allowed to relax at every point in the polarization curves.

Results and Discussion

End-On Model System. We started our investigations by calculating the end-on interaction of a lithium ion with the three mixed-valence complexes **1**−**3**. To mimic the polarization that occurs in one cell due to its neighboring cell, we placed a cation driver (lithium ion) on the same axis as both of the ruthenium atoms, and varied the driver−Ru(1) distance between about 8 and 20 Å. As the starting point, 8 Å was chosen because this is approximately the Ru−Ru distance in the pyrazine-bridged species (6.84 Å in X-ray structure[27]). As the outer point 20 Å was chosen because it would be reasonable to assume that if these complexes were aligned on a surface due to self-assembly, neighboring cells would likely be as close or closer than this. A lithium cation was chosen to function as the biasing charge, or driver, and is shown in Figure 4 along with the pyrazine-bridged complex. A cation was used because if this were a functioning QCA system the neighboring complex in a molecular wire would also be positively charged and these cell−cell interactions would drive the signal transfer. A plot of the Mulliken charge variation as the driver is moved is shown in Figure 4. The Mulliken charge on each ruthenium, as well as

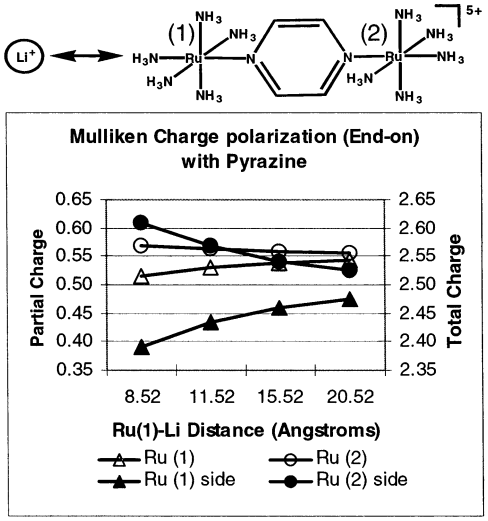

Figure 4. End-on polarization of the pyrazine-bridged complex by a lithium cation.

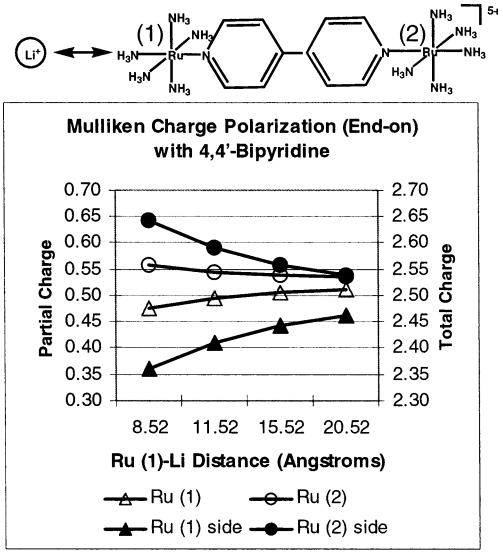

Figure 5. End-on polarization of the 4,4′-bipyridine-bridged complexes by a lithium cation.

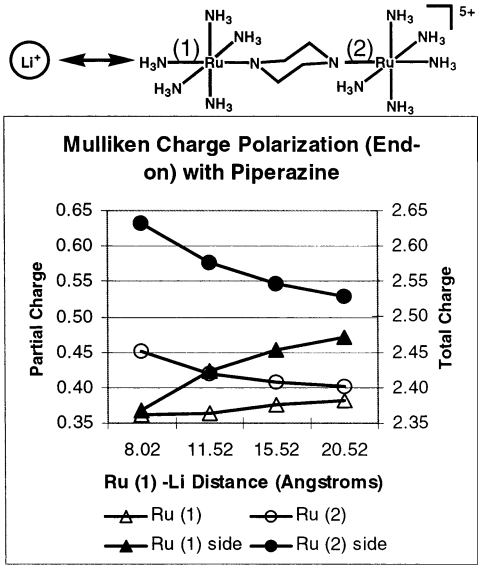

Figure 6. End-on polarization of the piperazine-bridged complexes by a lithium cation.

the total Mulliken charge on each side of the complex, is shown in the figures. The partial charge (ruthenium only) is shown in black curves with open triangles and circles. The corresponding axis is shown on the left of the graph. The total charge is depicted as black lines, with filled triangles and circles. The corresponding axis is on the right of the graph. To determine the total charge, the molecule was divided in half through the center of the bridging ligand, and the atomic charges on each side were added together to give these curves. The partial charge curves are not centered at 0.5 as one may at first expect, because some charge is also distributed on the bridging and ancillary ligands. Consequently, the partial charge curves are not necessarily symmetric. If the charge on the bridging and ancillary ligands is included (total charge), the curves become symmetric. The geometry was allowed to relax at each point on the graphs, although the geometry changes were quite small. Typically, the Ru(II) to the bridging ligand nitrogen-bond length fluctuated by less than 0.02 Å as the lithium cation was moved. Similarly, the Ru(III) to the bridging ligand nitrogen-bond length also fluctuated by less than 0.02 Å. As can be seen from Figures 4−6, the total charge is centered at 2.5.

The pyrazine-bridged complex is most polarized when the lithium ion is closest to the ruthenium. The same procedure was followed for the 4,4′-bipyridine- and piperazine-bridged complexes as well. The results are shown in Figures 5 and 6, respectively. Of the three complexes examined here, the pyrazine-bridged complex shows the least partial and total charge polarization of the three. The partial (total) Mulliken charge difference varies from approximately 0.01 (0.05) at 20 Å to 0.06 (0.22) at 8 Å. The charge varies very smoothly, as the lithium cation is moved farther away, due to the large amount of electronic communication between the two centers and extensive π bonding on the bridging ligand, which gives it the ability to delocalize charge throughout the complex. The 4,4′-bipyridine- and piperazine-bridged complexes exhibit very similar Mulliken charge differences, both larger than that for pyrazine. The partial (total) Mulliken charge difference for the 4,4′-bipyridine-bridged complex varies from approximately 0.02 (0.07) at 20 Å to 0.08 (0.28) at 8 Å. The partial (total) Mulliken charge difference for the piperazine-bridged complex varies from approximately 0.02 (0.06) at 20 Å to 0.09 (0.27) at 8 Å. In general for these complexes, there is a significant dropoff in polarization as the lithium ion is moved farther away. However, for the 4,4′-bipyridine-bridged complex the partial charge again varies smoothly, indicating the ability of the complex to delocalize the charge efficiently. The dihedral angle between the two rings of the 4,4′-bipyridine change little as the lithium ion is moved, ranging only from 34 to 40°. In contrast, the partial charge on the piperazine-bridged complex varies unevenly, likely due to the lack of electronic communication between the centers because of the use of a bridging ligand without π bonds. Overall, in terms of the shape of the curves, there is little difference between classes II and III, yet there are significant differences in the amount of polarization between these two classes, with class II displaying more polarization. Classes I and II display approximately the same amount of charge separation, but the shapes of the partial charge curves vary dramatically, from a smooth, nearly symmetrical polarization in the class II case to a very rough, unsymmetrical variation in the class I case. The shapes of the curves, especially the total charge curves, show a significant dropoff in polarization as the cation is moved farther away. The significant dropoffs in polarization indicate that an input, or driver, for QCA should be as close to the mixed-valence system as possible. The shapes of the curves are desirable for QCA, because it indicates a sharp

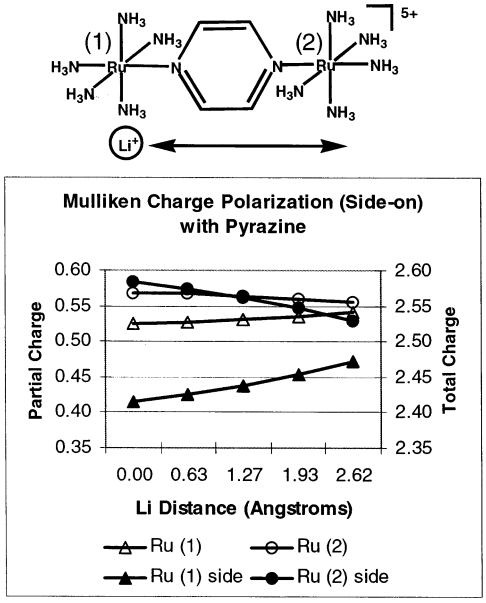

Figure 7. Side-on polarization of the pyrazine-bridged complexes by a lithium ion.

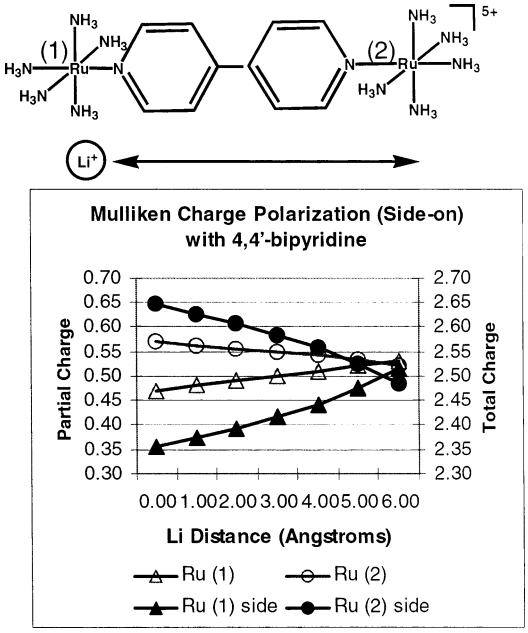

Figure 8. Side-on polarization of the 4,4′-bipyridine-bridged complexes by a lithium ion.

switching in the polarization, which causes less ambiguity between states than occurs with a gradual, linear response to the driver.

Side-on Model System. To mimic the polarization that would occur intramolecularly within a square complex (four ruthenium atoms), we placed a cation driver about 7.5 Å underneath but parallel to the Ru−Ru axis, and shuttled it along this axis. Again, a lithium cation was chosen to be the driver and is shown in Figure 7 along with the pyrazine-bridged mixed-valence system. The same procedure was followed for the 4,4′-bipyridine-bridged complex as well as for the piperazine-bridged complex, and the results are shown in Figures 8 and 9, respectively. The ideal behavior would be a curve with two plateaus that switches sharply between electronic configurations, true bistable character, unlike the gradual switching observed in Figures 7−9. The pyrazine-bridged complex again shows the least polarization of the three. The maximum Mulliken charge partial charge

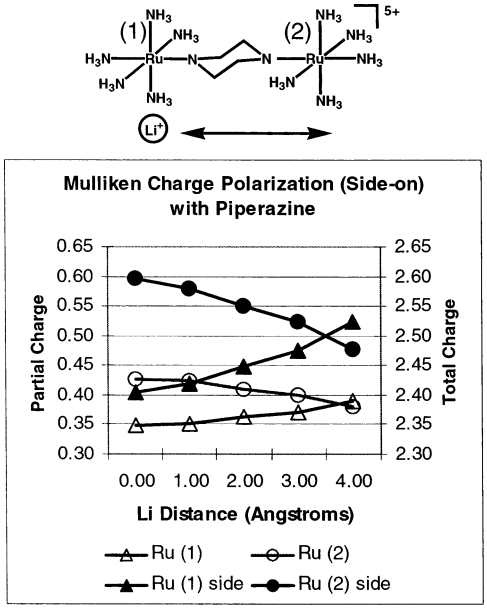

Figure 9. Side-on polarization of the piperazine-bridged complex by a lithium ion.

polarization between the ruthenium atoms is 0.04, while the maximum total charge difference is 0.17. The 4,4′-bipyridine-bridged complex exhibits a slightly larger partial charge difference, 0.10, and a much larger total charge difference, 0.29, than the piperazine-bridged complex. Again, the dihedral angle of the 4,4′-bipyridine varies little with movement of the lithium cation, from 27 to 31°. The piperazine-bridged complex shows a maximum partial charge difference of 0.08 and a maximum total charge difference of 0.19. The largest polarization occurs, as could be expected, when the lithium ion is directly underneath one of the ruthenium atoms. Once the lithium ion goes beyond the midpoint of the complex, the polarization curves cross. In all cases, a smooth, nearly linear response of the cell polarization to the position of the driver is obtained. This could, at least partially, be a result of the B3LYP functional used since this methodology is slightly biased toward delocalized structures. Again, the partial charge curves for the class II and III complexes vary smoothly as the driver is shuttled along its axis, while the partial charge curve for the class I complex is rough. This is probably due to the lack of electronic communication between the metal centers in the class I complex. The metal centers are not strongly coupled because of the lack of π bonds in the bridging ligand, which are useful for helping delocalize the charge throughout the complex. These results indicate that the class II complex is the best suited for QCA applications. Of the three classes, it exhibits the largest charge polarization in the side-on example, and almost exactly the same polarization as the class I complex in the end-on example, yet it has a very fast rate of electron transfer. Class II complexes have experimentally been shown to typically have electron-transfer rates between 10^6 and 10^{12} s^{-1},[7] which would be useful for doing fast computations.

Conclusions

These mixed-valence complexes show significant polarization when a biasing charge is added to the system. This type of analysis of the polarization of mixed-valence complexes will be useful in the design of complexes that are even better suited as QCA devices. The study could be extended to include different ancillary as well as bridging ligands to systematically

predict their effects on the polarization that can be achieved in the complexes. This will help identify what complexes will be useful before they are synthesized. The ability of these complexes to function as molecular switches will be influenced by the sensitivity of detectors that can be developed, as well as the overall charge dissipation as the electrostatic signal moves down the wire. Future studies should look at this signal dissipation by calculating molecular wires (formed by placing several of these complexes in a line) and observing how much the polarization decreases as the signal moves.

Acknowledgment. We gratefully acknowledge financial support from the National Science Foundation for a Graduate Fellowship to S.B., the Defense Advanced Research Projects Agency and the Office of Naval Research (DARPA/ONR N00014-99-1-0472), and generous allocation of computing resources from NCSA (University of Illinois at Urbana-Champaign), the Notre Dame Office of Information Technologies, and BoB, a Beowulf cluster at Notre Dame obtained through Grant DMR0079647 from the National Science Foundation.

Supporting Information Available: The Cartesian coordinates of all fully optimized complexes. This material is available free of charge via the Internet at http://pubs.acs.org.

References and Notes

(1) Lent, C. S.; Isaksen, B.; Lieberman, M. *J. Am. Chem. Soc.* **2003**, *125*, 1056−1063.

(2) Lieberman, M.; Chellamma, S.; Varughese, B.; Wang, Y.; Lent, C.; Bernstein, G. H.; Snider, G.; Peiris, F. C. *Ann. N. Y. Acad. Sci.* **2002**, *960*, 225−239.

(3) Orlov, A. O.; Amlani, I.; Bernstein, G. H.; Lent, C. S.; Snider, G. L. *Science* **1997**, *277*, 928−930.

(4) Glanz, J. *Science* **1995**, *269*, 1363−1364.

(5) Lau, V. C.; Berben, L. A.; Long, J. R. *J. Am. Chem. Soc.* **2002**, *124*, 9042−9043.

(6) Braun-Sand, S. B.; Wiest, O. *J. Phys. Chem. A* **2003**, *107*, 285−291.

(7) Robin, M. B.; Day, P. *Adv. Inorg. Chem. Radiochem.* **1967**, *10*, 247−422.

(8) Creutz, C.; Taube, H. *J. Am. Chem. Soc.* **1969**, *91*, 3988−3989.

(9) Creutz, C.; Taube, H. *J. Am. Chem. Soc.* **1973**, *95*, 1086−1094.

(10) Creutz, C.; Good, M. L.; Chandra, S. *Inorg. Nucl. Chem. Lett.* **1973**, *9*, 171−176.

(11) Creutz, C.; Taube, H. *Prog. Inorg. Chem.* **1983**, *30*, 1−73.

(12) Ferretti, A.; Lami, A.; Villani, G. *Inorg. Chem.* **1998**, *37*, 2799−2805.

(13) Sizova, O. V.; Baranovskii, V. I.; Panin, A. I.; Ivanova, N. V. *J. Struct. Chem.* **1999**, *39*, 471−479.

(14) Broo, A.; Larsson, S. *Chem. Phys.* **1992**, *161*, 363−378.

(15) Woitellier, S.; Launay, J. P.; Joachim, C. *Chem. Phys.* **1989**, *131*, 481−488.

(16) Frisch, M. J.; Trucks, G. W.; Schlegel, H. B.; Scuseria, G. E.; Robb, M. A.; Cheeseman, J. R.; Zakrzewski, V. G.; Montgomery, J. A., Jr.; Stratmann, R. E.; Burant, J. C.; Dapprich, S.; Millam, J. M.; Daniels, A. D.; Kudin, K. N.; Strain, M. C.; Farkas, O.; Tomasi, J.; Barone, V.; Cossi, M.; Cammi, R.; Mennucci, B.; Pomelli, C.; Adamo, C.; Clifford, S.; Ochterski, J.; Petersson, G. A.; Ayala, P. Y.; Cui, Q.; Morokuma, K.; Malick, D. K.; Rabuck, A. D.; Raghavachari, K.; Foresman, J. B.; Cioslowski, J.; Ortiz, J. V.; Stefanov, B. B.; Liu, G.; Liashenko, A.; Piskorz, P.; Komaromi, I.; Gomperts, R.; Martin, R. L.; Fox, D. J.; Keith, T.; Al-Laham, M. A.; Peng, C. Y.; Nanayakkara, A.; Gonzalez, C.; Challacombe, M.; Gill, P. M. W.; Johnson, B. G.; Chen, W.; Wong, M. W.; Andres, J. L.; Head-Gordon, M.; Replogle, E. S.; Pople, J. A. *Gaussian 98*: Gaussian, Inc.: Pittsburgh, PA, 1998.

(17) Bencini, A.; Gatteschi, D.; Mattesini, M.; Totti, F.; Ciofini, I. *Mol. Cryst. Liq. Cryst. A* **1999**, *335*, 1377−1386.

(18) Barone, V.; Bencini, A.; Ciofini, I.; Daul, C. A.; Totti, F. *J. Am. Chem. Soc.* **1998**, *120*, 8357−8365.

(19) Chen, Z.; Bian, J.; Zhang, L.; Li, S. *J. Chem. Phys.* **1999**, *111*, 10926−10933.

(20) Bencini, A.; Ciofini, I.; Daul, C. A.; Ferretti, A. *J. Am. Chem. Soc.* **1999**, *121*, 11418−11424.

(21) Wolfram Koch, M. C. H. *A Chemist's Guide to Density Functional Theory*; Wiley-VCH: Weinheim, 2000.

(22) Oxgaard, J.; Wiest, O. *J. Phys. Chem. A* **2001**, *105*, 8236−8240.

(23) Bally, T.; Borden, W. T. *Rev. Comput. Chem.* **1999**, *13*, 1−97.

(24) Hrouda, V.; Roeselova, M.; Bally, T. *J. Phys. Chem. A* **1997**, *101*, 3925−3935.

(25) Bally, T.; Sastry, G. N. *J. Phys. Chem. A* **1997**, *101*, 7923−7925.

(26) Jensen, F. *Introduction to Computational Chemistry*; John Wiley & Sons: Chichester, 1998.

(27) Beattie, J. K.; Hush, N. S.; Taylor, P. R.; Raston, C. L.; White, A. H. *J. Chem. Soc., Dalton Trans.* **1977**, 1121−1124.